Thermal Spray: Practical Solutions for Engineering Problems, C. C. Berndt (Ed.), Published by ASM International, Materials Park, Ohio-USA, 1996

Mathematical Modeling of Flattening Process on Rough Surfaces in Thermal Spray

H. Fukanuma
Plasma Giken Co., Ltd., Saitama, Japan

Abstract

Thermal spray layers are formed on rough surfaces; however, the flattening process on rough surfaces has not yet been clarified. A mathematical flattening model which takes into account the roughness of the substrate or previously coated layers is proposed in this paper. As a result of surface roughness, the flattening degree and the flattening time decrease with increasing surface roughness in this model. In addition, the characterization of surface roughness is introduced for the flattening model. Several calculated cases of the flattening model are shown.

THE FLATTENING PROCESS of impinged molten particles onto substrates affects the mechanical and physical properties of thermal sprayed coatings. The flattening process is one of the most important processes in thermal spraying, as it helps one to understand the physics of thermal spray and the characteristics of the sprayed layers. Many flattening models of molten or liquid particle impingement on flat surfaces have been proposed [1-6]. These mathematical models were concerned with the flattening processes on smooth surfaces. In addition to these models, many experimental investigations of splat formation on both smooth and rough surfaces have been reported [7-16].

Flattening processes on rough surfaces have been investigated recently. Moreau et al [14] have shown that the flattening degree and the flattening time of molybdenum splats on both roughened glass and molybdenum surfaces were less than on smooth surfaces. Leger et al [15] have shown that the flattening degree of zirconia splats on roughened steel surfaces decreases with increasing roughness in a relationship between the flattening degree and the Reynolds number. Bianchi et al [16] have shown that splat morphology on rough surfaces is different from that on smooth surfaces.

How does the surface roughness influence the flattening process in thermal spray coatings? First of all, we must consider the geometry of the surface roughness. Let's consider an idealized roughened surface as shown in Fig. 1-a. The cones which have height a and bottom radius b are aligned with distance l between the bottom centers of adjacent cones on the smooth, flat surface.

We can assume that an impinging molten particle begins to spread in the radial direction as a thin disk of thickness h at the impinging point of the particle onto the substrate, and that the thickness h is constant during flattening as shown in Fig. 2.

We assume that a molten particle impacts onto the idealized rough surface, and we classify the roughness into three cases: (1) the cone's height a is much larger than the disk thickness h, (2) the cone's height is much smaller than the disk thickness, and (3) the cone's height is approximately equal to the disk thickness.

In the spreading process in case (1), it can be considered that the fluid in the impinging particle, mostly flows along the valleys because the fluid has a velocity component perpendicular to the surface. A part of the fluid encountering the mountains climbs the slopes, then the liquid probably flies off the mountain, and a splash occurs if the radial velocity is large enough compared to the fluid surface tension. On the other hand, the fluid probably travels around the mountains and goes down the valleys if the radial velocity is not large enough for the fluid to climb over the mountains. The perpendicular velocity is largest at the disk center and is smaller farther from the center. If the impinging velocity is large and roughness is much large compared to the splat thickness, splashing possibly begins at impact and some of the fluid splashes away. This is because the radial velocity at impact is 2 - 5 times the impinging velocity, as shown by Heymann [2] and will be shown in this article, so the radial flow can climb and fly off the mountains in the short time after impact. Thereafter, because the following radial velocity rapidly decreases, and the velocity near the top of the particle becomes quite small when it comes to the surface, the small splat remains.

The mountains' geometric shapes influence the splash

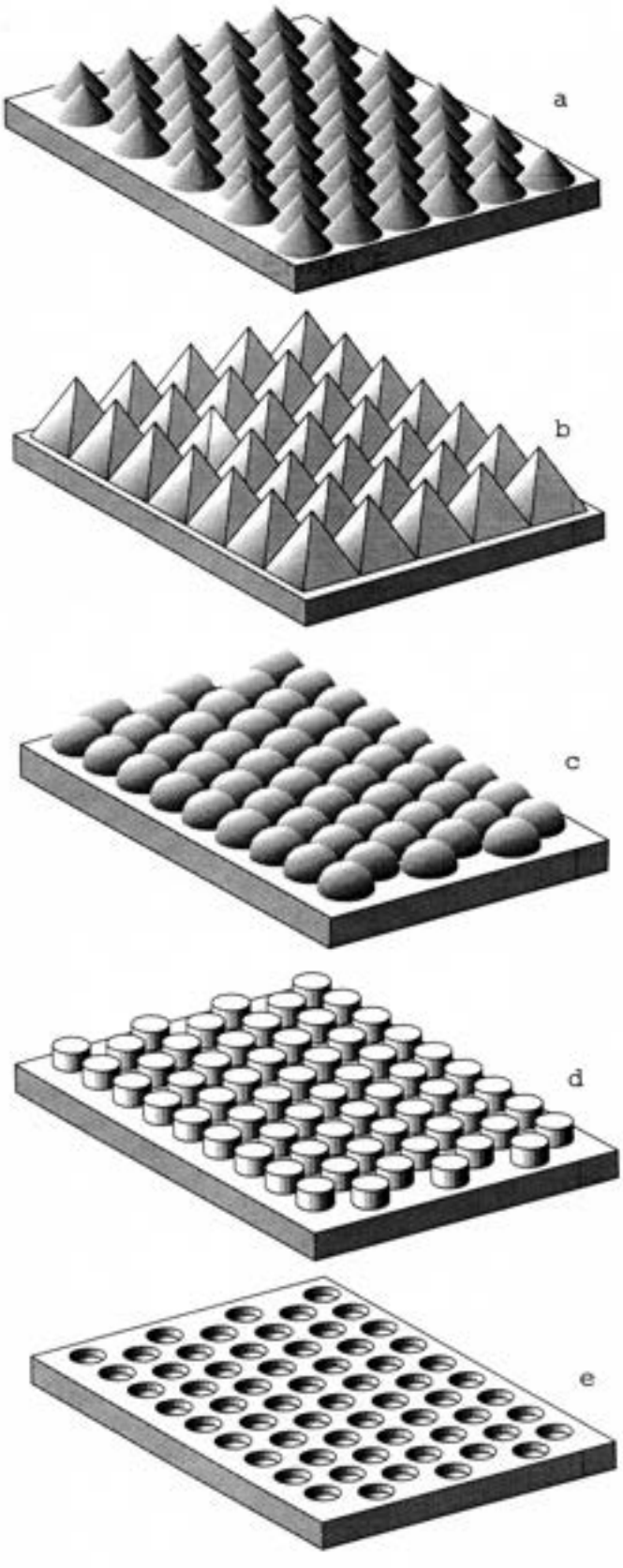

Fig.1 Schematic of several kinds of idealized rough surfaces.

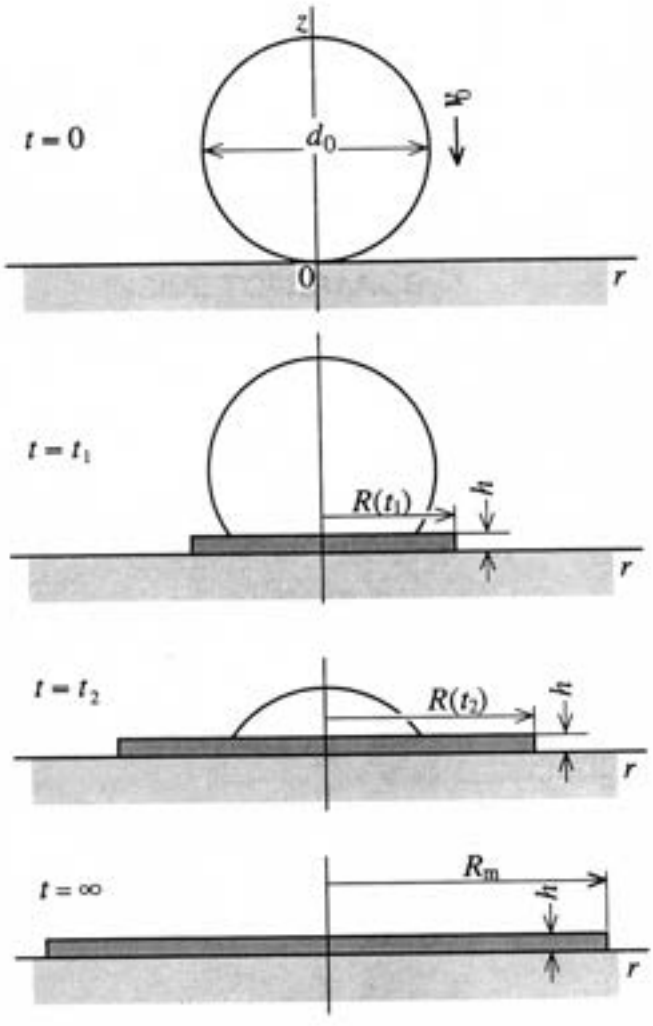

Fig.2 Schematic of the flattening process.

phenomena. For example, the pyramid mountain as shown in Fig. 1-b causes much more splash than the cone mountain, because the flat slope area can carry more fluid than the cone. If the mountains' arrangement is symmetrical to the axis perpendicular to the surface through the particle center, the splat shape is also symmetrical, but the rim line is both convex and concave. If the particle impinges directly onto the top of the high large mountain, splashing occurs easily, because radial flow is caused at the upper part of the particle and the radial flow direction becomes upward as shown in Fig. 3. The actual surface roughness of a blasted substrate or previously sprayed layer is much more complicated than these ideal models, and thus the actual splats will be irregular. The splashing and the splat morphology strongly depend on the topography of the rough surface. When we solve the flattening process in this case, we must consider the interaction of the flowing fluid and every mountain. It is almost impossible to construct the equations to solve the problem, and to find the conditions which cause splashing.

In case (2), flattening processes do not cause splashing because the small mountains cannot produce the velocity or

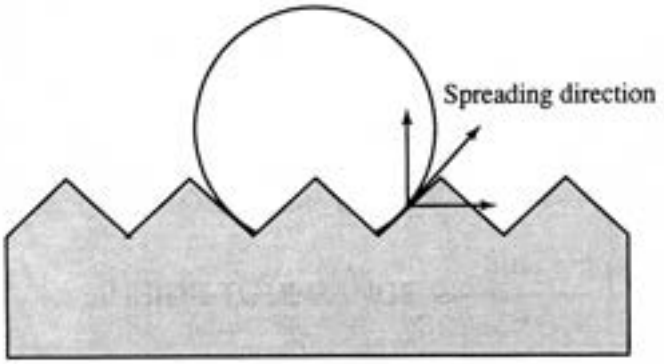

Fig. 3 Schematic of the cross section at impact on a large mountain surface.

the force in the vertical directions that is necessary to cause the fluid to take off from the surface. This is similar to a deep river flowing on a slightly rough river bed. In this case, it is satisfactory to consider the flattening process to be like the one on flat surfaces.

In case (3), the spreading phenomena are explained by case (1) or (2) depending on the impinging and surface conditions. If the radial velocity is not large, splashing probably does not take place. If splashing should occur, it is weak. If radial velocity is large, or the mountain slopes' angle makes the flow velocity in parallel to the slopes large enough for the flow to fly off the surface, then splashing occurs.

In addition to surface roughness, the wetability between a splat and the substrate or a previously sprayed layer greatly affects the flattening process, in particular the splashing process. Even if the surface is smooth, splashing can occur as a splat does not wet the substrate at all, or very slightly. The influence of wetabilty is not considered in this paper.

Modeling

This study refers to the modeling on a rough surface in case (2). It is difficult to take the roughness into considerations in case (1), because of the lack of understanding of the characterization and the topography of such rough surfaces. Also, we need to clarify the particle impact process onto rough surfaces at the moment of collision. It is also difficult to treat case (3); however, in a case without splashing, we might treat that as an extension of case (2).

It is nearly impossible to consider the interaction between the expanding splat and every mountain in the flattening process on a rough surfaces. A better way is to take the average of the fluid flow field on a small area of rough surface in order to characterize the flow field in the valleys. The flow field of the lower fluid as shown in Fig. 4, which flows in the valleys is very different from the flow field of the upper fluid, which flows over the tops of the mountains. The lower fluid flows much less than the upper fluid because the mountains impede the lower part of the fluid flow. If the lower flow has negligible affect on the upper flow, we can classify the fluid of

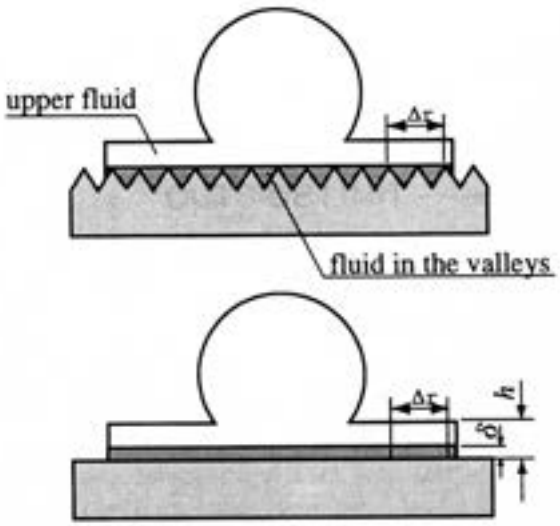

δ equal to the average depth of fluid in the valleys

Fig. 4 Schematic of the valley fluid converting to that on a smooth surface

the disk into two parts: the fluid that flows in the valleys and the fluid that flows over the mountains. We assume that the flow field in the valleys between r and $r+\Delta r$, although complicated, can be represented by the flow field in the fluid area $\Delta r \times \delta$, where δ is obtained by taking the average of the fluid depth in the valleys. The entire fluid in the valleys can be expressed as a thin disk by adding all elements in Δr from the center to outer rim of the splat. Thus, the flattening model can be represented by two disk layers on a smooth surface instead of the complicated splat on the roughened surface.

How do we characterize the surface roughness which affects the flattening process? We can introduce two parameters which influence the splat spreading process on the rough surface: one parameter is the volume of the valley space contained in a unit area on the surface, the other is a parameter which gives an expression of the fluid's "flowability" in the valley.

The volume of the valleys is a function of the mountains' height, shape, and arrangement. In the case of the cones surface in Fig. 1-a, because the valley volume ψ is a function of a cone height a, radius of cone bottom circle b and distance l between the bottom centers of adjacent cones, the volume can be obtained on unit surface area as

$$\psi = \left(1 - \frac{\pi}{6\sqrt{3}} \frac{b^2}{l^2}\right) a \qquad [1]$$

When $b = l$, for example, when the bottom circle rims contact each other, we obtain $\psi = (1 - 0.302)a$. We can similarly obtain the volume in an idealized case in which i depends on surface topography. Then, Eq. 1 is expressed as

$$\psi = (1 - i)a \qquad [2]$$

where i is a parameter which is smaller than 1, since $b \le l$. The volume Ψ is expressed as the product of mountain height and a coefficient as shown Eq. 2. Substituting $(1-i)=j$ into Eq. 2, the expression becomes

$$\Psi = j \times a \qquad [3]$$

Valley volume Ψ can be expressed by two parameters j and a. In general, j is smaller than 1, since $0 \le i \le 1$.

On the other hand, determining the parameter which expresses fluid mobility depends on the shape of the mountains and their arrangement. We consider that the flow field in the splat is represented in cylindrical coordinates $(0,r,\theta,z)$, and if the flow field in a splat on a smooth, flat surface is $U(U_r,U_\theta,U_z)$, we assume that the flow field in the valleys on a rough surface is $k \times U_r$, where k is a coefficient smaller than 1. The flow on a smooth surface is expressed when $k=1$. We have now converted the problem of the flattening process on rough surfaces into the flattening process on smooth, flat surfaces by introducing parameters which characterize the rough surface. The parameters are a, j, and k instead of a and Ψ.

In Fig. 5, we assume the energy dissipation in region I is negligible, because the velocity gradient is most likely small. If the velocity gradient is large in that part, the spherical part on the disk will change shape. The splat formation pictures in the work by Engel [1] and in the previous work by Ohmori and myself [6], however, show that the shape of the spherical part keeps its sphericity quite well. Thus, we consider the flow field in just the disk (region II and III). We can assume the radial flow field U_r in the disk is:

$$U_r = kC_1 e^{-\alpha t} rz(2\delta - z), \quad \text{when } 0 \le z < \delta,\ 0 \le r < R_0 \qquad [4]$$

$$U_r = C_1 e^{-\alpha t} r\left[(z-\delta)\{2(h-\delta)-(z-\delta)\}+k\delta^2\right], \quad \text{when } \delta \le z < h,\ 0 \le r < R_0 \qquad [5]$$

$$U_r = kC_2 e^{-\alpha t}\frac{z(2\delta - z)}{r}, \quad \text{when } 0 \le z < \delta,\ R_0 \le r \qquad [6]$$

$$U_r = C_2 e^{-\alpha t}\frac{(z-\delta)\{2(h-\delta)-(z-\delta)\}+k\delta^2}{r}, \quad \text{when } \delta \le z < h,\ R_0 \le r \qquad [7]$$

where U_r is the radial flow component, C_1, C_2 and α are constants, t is the time after the impact, h is the disk thickness, δ is the average thickness of the fluid in the valleys, and k is the parameter which indicates fluid mobility in the valleys. Equation 4 and 5 are r-component of the fluid field in lower and upper part of region II, respectively, and Eq. 6 and 7 are r-component of the fluid field in lower and upper part of region III, respectively. We assume $R_0 = d_0/2$, where d_0 is the particle diameter at impact.

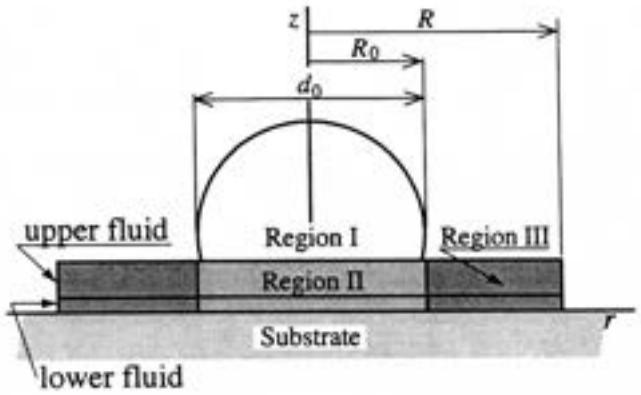

Fig. 5 Schematic of the particle regions in which fluid flows are different.

The θ-component flow U_θ equals 0, because the flow field should be symmetrical around the z-axis. The internal friction in the perpendicular direction is negligible, because the disk is so thin that the energy dissipated by the velocity gradient in the perpendicular direction is negligible compared to that in the radial direction.

The assumed flow field shows that the radial flow velocity will increase proportionally to the square of the height from the fluid bottom, and will increase proportionally to the radius from the center to a certain radius R_0, and will decrease inversely to the radius from R_0 to the outer rim. We call these region II and III, respectively, as shown in Fig. 5. The formulas are chosen so that the velocity gradient is equal to zero on the top surfaces of region II and III. The flow field will depend on time with an exponential $\exp(-\alpha t)$, after taking into consideration the fact that the spreading rate rapidly decreases with the passage of time [6].

The disk volume of radius $R(t)$ and thickness h at time t after impact is expressed as

$$\pi h R^2 = \pi h R_0^2 + 2\pi R_0 \int_{t_0}^{t}\int_0^h U_r\, dz\, dt \qquad [8]$$

where R_0 is the disk radius at time t_0. The integration on the right hand side represents the fluid volume which flows out from region II into region III through the boundary at R_0 during the time between t_0 and t. Substituting the sum of Eq. 6 and 7 into Eq. 8, the expression becomes

$$\pi h R^2 = \pi h R_0^2 + 2\pi R_0 \int_{t_0}^{t}\int_0^h \left[kC_2 e^{-\alpha t}\frac{z(2\delta - z)}{r} + C_2 e^{-\alpha t}\frac{(z-\delta)\{2(h-\delta)-(z-\delta)\}+k\delta^2}{r}\right] dz\, dt$$
$$= \pi h R_0^2 + \frac{4}{3}\pi C_2\left\{(h-\delta)^3 + \frac{3}{2}k\delta^2\left(h-\frac{1}{3}\delta\right)\right\} \times \frac{e^{-\alpha t_0} - e^{-\alpha t}}{\alpha} \qquad [9]$$

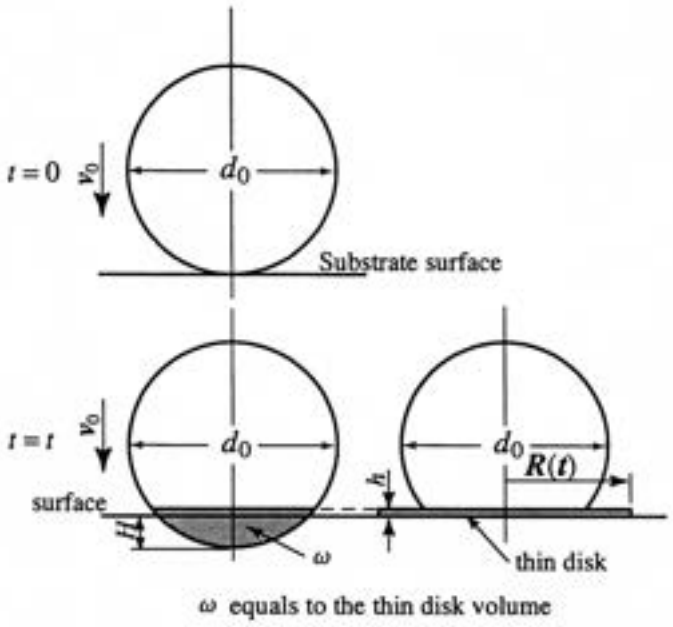

Fig. 6 Schematic of the bottom part of a spherical particle changing to a thin disk.

We obtain the disk radius as a function of time by solving Eq. 9 for R, and finding coefficients C_2, α and the disk thickness h. Coefficients C_1, C_2 and α are found by solving the equations of the boundary conditions. The boundary conditions are:

(i) when a thin disk of thickness h begins to spread at the impact point in the radial direction parallel to the surface, and the particle keeps moving perpendicular to the surface at the impact velocity v_0 for a time after impingement, the fluid volume ω in Fig. 6 is expressed as

$$\omega = \int_0^{H+h} \pi r^2 dz \qquad [10]$$

where r is the circle radius given by cutting the particle by planes parallel to the substrate surface, and H is the particle's moving distance during time t (i.e. $H = v_0 t$ in the short time after impact). Since the fluid volume ω converts to the thin disk, namely $\omega = \pi h R^2$, the next equation holds.

$$\pi h R^2 = \pi\left[\frac{1}{2}d_0(H+h)^2 - \frac{1}{3}(H+h)^3\right] \qquad [11]$$

Differentiating Eq. 11 by t, and since $(H+h)/d_0 << 1$, the radial expanding rate of the disk can be expressed as

$$\frac{dR}{dt} = v_0\sqrt{\frac{d_0}{2h}}\frac{1-\dfrac{(H+h)}{d_0}}{\sqrt{1-\dfrac{2}{3}\dfrac{(H+h)}{d_0}}}$$

$$\cong v_0\sqrt{\frac{d_0}{2h}}\left(1-\frac{2}{3}\frac{(H+h)}{d_0}\right) \cong v_0\sqrt{\frac{d_0}{2h}}\left(1-\frac{2}{3}\frac{v_0 t}{d_0}\right) \qquad [12]$$

where d_0 is the particle diameter at the time of collision. Assuming $t_0 \cong 0$, we obtain

$$\left(\frac{dR}{dt}\right)_{t=t_0} = v_0\sqrt{\frac{d_0}{2h}} \qquad [13]$$

Differentiating Eq. 9 by t, the expression becomes

$$\frac{dR}{dt} = \frac{\dfrac{4}{3}C_2\left\{(h-\delta)^3 + \dfrac{3}{2}k\delta^2\left(h-\dfrac{1}{3}\delta\right)\right\}e^{-\alpha t}}{2hR} \qquad [14]$$

When $t = t_0$, Eq. 14 becomes

$$\left(\frac{dR}{dt}\right)_{t=t_0} = \frac{\dfrac{4}{3}C_2\left\{(h-\delta)^3 + \dfrac{3}{2}k\delta^2\left(h-\dfrac{1}{3}\delta\right)\right\}e^{-\alpha t_0}}{2hR_0} \qquad [15]$$

We obtain the next equation from Eq. 13 and 15.

$$C_2 = \frac{3}{2}\frac{hv_0R_0}{\left\{(h-\delta)^3 + \dfrac{3}{2}k\delta^2\left(h-\dfrac{1}{3}\delta\right)\right\}}\sqrt{\frac{d_0}{2h}} \qquad [16]$$

(ii) Because the fluid volume which flows out through the boundary between region II and III is the same as the fluid volume which flows into region III, the next equation holds.

$$\begin{aligned} &2\pi R_0\left[\int_0^{\delta} kC_1e^{-\alpha t}(2\delta - z)rzdz\right. \\ &\left.+\int_0^{\delta} C_1e^{-\alpha t}r\left[(z-\delta)\left\{2(h-\delta)-(z-\delta)\right\}+k\delta^2\right]dz\right] \\ &= 2\pi R_0\left[\int C_2e^{-\alpha t}\frac{z(2\delta-z)}{r}dz\right. \\ &\left.+\int_{\delta}^{h} C_2e^{-\alpha t}\frac{(z-\delta)\left\{2(h-\delta)-(z-\delta)\right\}+k\delta^2}{r}dz\right] \end{aligned} \qquad [17]$$

Solving Eq. 17, we obtain

$$C_1R_0 = C_2 \qquad [18]$$

(iii) At $t=\infty$, the radius becomes $R=R_m$. Substituting $t=\infty$, $t_0=0$ and $R=R_m$ into Eq. 9, we obtain

$$\alpha=\frac{4}{3}\frac{C_2}{h}\frac{\left\{(h-\delta)^3+\frac{3}{2}k\delta^2\left(h-\frac{1}{3}\delta\right)\right\}}{R_m{}^2-R_0{}^2} \qquad [19]$$

From Eq. 16, 18 and 19, we obtain

$$C_1=\frac{3}{2}\frac{hv_0}{R_0\left\{(h-\delta)^3+\frac{3}{2}k\delta^2\left(h-\frac{1}{3}\delta\right)\right\}}\sqrt{\frac{d_0}{2h}} \qquad [20]$$

$$C_2=\frac{3}{2}\frac{hv_0R_0}{\left\{(h-\delta)^3+\frac{3}{2}k\delta^2\left(h-\frac{1}{3}\delta\right)\right\}}\sqrt{\frac{d_0}{2h}} \qquad [21]$$

$$\alpha=\frac{2R_0v_0}{R_m{}^2-R_0{}^2}\sqrt{\frac{d_0}{2h}} \qquad [22]$$

Substituting Eq. 20, 21 and 22 into Eq. 9, and then substituting $t_0=0$ into the equation and directing our attention to the relationships $R=D/2$, $R_0=d_0/2$, $R_m=D_m/2$ and $h=d_0{}^3/6R_m{}^2$, we obtain an equation which expresses the splat diameter expanding as a function of time as follows,

$$\frac{D}{d_0}=\frac{D_m}{d_0}\sqrt{1-\left(1-\frac{d_0{}^2}{D_m{}^2}\right)\exp\left(-\frac{2\sqrt{3}}{\left(1-\frac{d_0{}^2}{D_m{}^2}\right)}\frac{d_0}{D_m}\frac{v_0}{d_0}t\right)} \qquad [23]$$

If $d_0{}^2/D_m{}^2 \ll 1$, Eq. 23 is simplified as

$$\frac{D}{d_0}=\frac{D_m}{d_0}\sqrt{1-\exp\left(-2\sqrt{3}\frac{d_0}{D_m}\frac{v_0}{d_0}t\right)} \qquad [24]$$

The unknown is still D_m in Eq. 23 and 24. If we find D_m the problem has been solved. The parameter k, j and a do not appear in Eq. 23 and 24. They must be hidden in D_m.

Let's find D_m. The next equation holds because of the conservation of energy.

$$\frac{1}{2}\rho\frac{4}{3}\pi\left(\frac{d_0}{2}\right)^3 v_0{}^2=\int_0^\infty\int_V\mu\left(\frac{\partial U_r}{\partial z}\right)^2 dVdt$$
$$+\gamma\left[\frac{1}{3}\pi\left(\frac{d_0}{2}\right)^2-2\pi\left(\frac{D_m}{2}\right)^2\right] \qquad [25]$$

where μ and γ are the viscosity coefficient and the surface tension of the fluid, respectively. In Eq. 25, the left hand side is the particle kinetic energy at impact, the integration is the dissipate energy of friction by shear stress in the fluid, and the second term on the right hand side is the increase in surface energy due to the increase in splat surface area during the flattening process. Substituting Eq. 4, 5, 6 and 7 into the integration term in Eq. 25, and since the volume element dV is equal to $rdrd\theta dz$ in cylindrical coordinates, the expression becomes

$$\int_0^\infty\int_V\mu\left(\frac{\partial U_r}{\partial z}\right)^2 dVdt$$
$$=\int_0^\infty\int_0^{R_0}\int_0^{2\pi}\int_0^{\delta}\mu\left(\frac{\partial}{\partial z}kC_1e^{-\alpha t}rz(2\delta-z)\right)^2 rdrd\theta dzdt$$
$$+\int_0^\infty\int_0^{R_0}\int_0^{2\pi}\int_0^{\delta}\mu\left(\frac{\partial}{\partial z}C_1e^{-\alpha t}\right.$$
$$\left.\times r\left[(z-\delta)\left\{2(h-\delta)-(z-\delta)\right\}+k\delta^2\right]\right]^2 rdrd\theta dzdt$$
$$+\int_{t_0}^\infty\int_{R_0}^{R}\int_0^{2\pi}\int_\delta^{h}\mu\left(\frac{\partial}{\partial z}kC_2e^{-\alpha t}\frac{z(2\delta-z)}{r}\right)^2 rdrd\theta dzdt$$
$$+\int_{t_0}^\infty\int_{R_0}^{R}\int_0^{2\pi}\int_\delta^{h}\mu\left(\frac{\partial}{\partial z}C_2e^{-\alpha t}\right.$$
$$\left.\times\frac{(z-\delta)\left\{2(h-\delta)-(z-\delta)\right\}+k\delta^2}{r}\right)^2 rdrd\theta dzdt \qquad [26]$$

Solving Eq. 26 after substituting Eq. 20, 21 and 22 into Eq. 26, the expression becomes

$$\int_0^\infty\int_V\mu\left(\frac{\partial U_r}{\partial z}\right)^2 dVdt$$
$$=\frac{9\sqrt{3}}{64}\frac{\pi\mu v_0D_m{}^5}{d_0{}^3}\frac{\left(-\frac{1}{2}+\frac{d_0{}^2}{2D_m{}^2}+\ln\frac{D_m}{d_0}\right)}{\left(1-\frac{d_0{}^2}{D_m{}^2}\right)}$$
$$\times\frac{\left\{\left(1-\frac{\delta}{h}\right)^3+\frac{k^2\delta^3}{h^3}\right\}}{\left\{\left(1-\frac{\delta}{h}\right)^3+\frac{3}{2}\frac{k\delta^2}{h^2}\left(1-\frac{1}{3}\frac{\delta}{h}\right)\right\}^2} \qquad [27]$$

Substituting Eq. 27 into Eq. 25, the expression becomes

$$\frac{1}{2}\rho\frac{4}{3}\pi\left(\frac{d_0}{2}\right)^3 v_0^2$$

$$= \frac{9\sqrt{3}}{64}\frac{\pi\mu v_0 D_m^5}{d_0^3}\frac{\left(-\frac{1}{2}+\frac{d_0^2}{2D_m^2}+\ln\frac{D_m}{d_0}\right)}{\left(1-\frac{d_0^2}{D_m^2}\right)} \times \frac{\left\{\left(1-\frac{\delta}{h}\right)^3+\frac{k^2\delta^3}{h^3}\right\}}{\left\{\left(1-\frac{\delta}{h}\right)^3+\frac{3}{2}\frac{k\delta^2}{h^2}\left(1-\frac{1}{3}\frac{\delta}{h}\right)\right\}^2}$$

$$+\gamma\left[\frac{1}{3}\pi\left(\frac{d_0}{2}\right)^2-2\pi\left(\frac{D_m}{2}\right)^2\right] \qquad [28]$$

When surface energy is negligible, Eq. 28 is simplified as

$$\frac{\rho v_0 d_0}{\mu} = \left[\frac{27\sqrt{3}}{16}\frac{D_m^5}{d_0^5}\frac{\left(-\frac{1}{2}+\frac{d_0^2}{2D_m^2}+\ln\frac{D_m}{d_0}\right)}{\left(1-\frac{d_0^2}{D_m^2}\right)}\right] \times \frac{\left\{\left(1-\frac{\delta}{h}\right)^3+\frac{k^2\delta^3}{h^3}\right\}}{\left\{\left(1-\frac{\delta}{h}\right)^3+\frac{3}{2}\frac{k\delta^2}{h^2}\left(1-\frac{1}{3}\frac{\delta}{h}\right)\right\}^2} \qquad [29]$$

Approximating the term in brackets on the right hand side in Eq. 29, and substituting $\rho v_0 d_0/\mu = \mathrm{Re}$ into Eq. 29, the expression becomes

$$\mathrm{Re} = \left(\frac{1}{1.06}\right)^6\left(\frac{D_m}{d_0}\right)^6 \frac{\left\{\left(1-\frac{\delta}{h}\right)^3+\frac{k^2\delta^3}{h^3}\right\}}{\left\{\left(1-\frac{\delta}{h}\right)^3+\frac{3}{2}\frac{k\delta^2}{h^2}\left(1-\frac{1}{3}\frac{\delta}{h}\right)\right\}^2} \qquad [30]$$

Substituting $h = 2d_0^3/3D_m^2$ into Eq. 30, the expression becomes

$$\mathrm{Re} = \left(\frac{1}{1.06}\right)^6\left(\frac{D_m}{d_0}\right)^6 \times \frac{\left\{\left(1-\frac{3}{2}\frac{D_m^2}{d_0^2}\frac{\delta}{d_0}\right)^3+k^2\left(\frac{3}{2}\frac{D_m^2}{d_0^2}\frac{\delta}{d_0}\right)^3\right\}}{\left\{\left(1-\frac{3}{2}\frac{D_m^2}{d_0^2}\frac{\delta}{d_0}\right)^3+\frac{2}{3}k\left(\frac{3}{2}\frac{D_m^2}{d_0^2}\frac{\delta}{d_0}\right)^2\left(1-\frac{1}{2}\frac{D_m^2}{d_0^2}\frac{\delta}{d_0}\right)\right\}^2} \qquad [31]$$

Since the fluid volume Ψ in valleys on unit area equals the average depth δ of the fluid in valleys on unit surface area, namely $\delta = \Psi = j\cdot a$, substituting $\delta = j\cdot a$ into Eq. 31, the expression becomes

$$\mathrm{Re} = \left(\frac{1}{1.06}\right)^6\left(\frac{D_m}{d_0}\right)^6 \times \frac{\left\{\left(1-\frac{3}{2}\frac{D_m^2}{d_0^2}\frac{ja}{d_0}\right)^3+k^2\left(\frac{3}{2}\frac{D_m^2}{d_0^2}\frac{ja}{d_0}\right)^3\right\}}{\left\{\left(1-\frac{3}{2}\frac{D_m^2}{d_0^2}\frac{ja}{d_0}\right)^3+\frac{2}{3}k\left(\frac{3}{2}\frac{D_m^2}{d_0^2}\frac{ja}{d_0}\right)^2\left(1-\frac{1}{2}\frac{D_m^2}{d_0^2}\frac{ja}{d_0}\right)\right\}^2} \qquad [32]$$

We have obtained the equation expressing the relationship between Reynolds number and flattening ratio $D(t=\infty)=D_m$. the equation includes the parameters characterizing surface roughness. If $k=0$, that is, the fluid cannot flow in the valleys, Eq. 32 is simplified as

$$\mathrm{Re} = \frac{\left(\frac{1}{1.06}\right)^6\left(\frac{D_m}{d_0}\right)^6}{\left(1-\frac{3}{2}\frac{D_m^2}{d_0^2}\frac{ja}{d_0}\right)^3} \qquad [33]$$

Solving Eq. 32 or 33 for D_m/d_0 and substituting the solution into Eq. 23 or 24, we obtain the deformation ratio of the expanding splat diameter to the particle diameter at impact as a function of time. In particular, since Eq. 33 is a cubic equation of $(D_m/d_0)^2$, the equation can be solved. Furthermore, if $D_m^2/d_0^2\cdot ja/d_0 << 1$, the simplified solution is found as follows,

$$\frac{D_m}{d_0} = 1.06\,\mathrm{Re}^{\frac{1}{6}} \times \sqrt{\frac{\left(\frac{1}{2}+\sqrt{\frac{1}{4}+\left(\frac{3}{2}\frac{ja}{d_0}\right)^3(1.06)^6\,\mathrm{Re}}\right)^{\frac{2}{3}}-\frac{3}{2}\frac{ja}{d_0}(1.06)^2\,\mathrm{Re}^{\frac{1}{3}}}{\left(\frac{1}{2}+\sqrt{\frac{1}{4}+\left(\frac{3}{2}\frac{ja}{d_0}\right)^3(1.06)^6\,\mathrm{Re}}\right)^{\frac{1}{3}}}} \qquad [34]$$

Equation 34 is the simplified formula of deformation ratios on rough surfaces at $k=0$.

If $(3ja/2d_0)^3\,\mathrm{Re}$ is negligibly small, Eq. 34 becomes

$$\frac{D_m}{d_0} = 1.06\,\mathrm{Re}^{\frac{1}{6}}\sqrt{1-\frac{3}{2}\frac{ja}{d_0}(1.06)^2\,\mathrm{Re}^{\frac{1}{3}}} \qquad [35]$$

We obtain more simplified solution of the flattening ratio. This equation holds when surface roughness is much small compared to the particle diameter at impact.

The equation by substituting the solution of Eq. 32, 33, 34 or 35 into Eq. 23 or 24 expresses the flattening ratios of the expanding splat with passage of time on rough surfaces.

Numerical results and discussion

Some numerical results of this model show how roughness affects flattening processes, such as, the influence of surface roughness to flattening time and flattening ratios. The case of a molten nickel particle will be shown and the conditions at impact are shown in Table 1.

Table 1 Physical properties of a molten nickel particle at given impact velocity.

Material	impact velocity [m/sec]	particle diameter [μm]	particle density [kg/m^3]	viscosity coefficient [mPa·s]	Re
Ni	100	50	7905	4.9	8066

The flattening ratios of a spreading nickel splat with different conditions of the rough surface with time are shown in Fig. 7. It shows that flattening ratios and spreading rates become smaller with increasing surface roughness, which the parameter a represents. The parameter a greatly affects the flattening ratio and flattening time compared to parameter k, which represents fluid mobility in valleys on rough surfaces as shown Fig. 8 and 9. It is noted that the product of a and j influences the flattening process, not a or j alone, as shown in Eq. 32, 33, 34 or 35. Figure 8 shows the relationship between the mountain height of surface roughness a and the flattening time $t_{0.9}$ when the splat diameter $D(t)$ reaches $0.9\,D_m$. The time $t_{0.9}$ is obtained by substituting $D=0.9D_m$ into Eq. 24 followed by solving for t as follows,

$$t_{0.9}=-\frac{1}{2\sqrt{3}}\frac{D_m}{d_0}\frac{d_0}{v_0}\log\left(1-0.9^2\right) \qquad [36]$$

The graph shows that the flattening time decreases with increasing roughness. The influence of the parameter k on the flattening time is less than that of the parameter a. The flattening time is 1.14 μsec on a smooth, flat surface when a 50 μm nickel particle impinges at velocity of 100 m/sec; however, it is 0.86 μsec on a rough surface of 2.2 μm and fluid mobility of $k=0$ as shown in Fig. 8. The deviation of flattening time on a rough surface from that on the smooth surface is approximately 25% less and indicate that a greatly affects the flattening time.

Figure 9 shows that the flattening ratio is affected strongly by the parameter of mountain height a on a rough surface, but affected weakly by the parameter of flowability k. Figure 10 shows that the increasing rates of flattening ratios with Reynolds number become smaller with increasing roughness. The flattening ratio is strictly a function of a/d_0 and Re, not directly of a as shown in Eq. 32, 33, 34 and 35. Surface roughness is related to the impinging particle diameter or strictly to the splat thickness, because a larger particle expands with a thicker splat compared to a smaller one with other conditions the same.

When we consider applying this model to very rough surfaces, although actual rough surfaces are much more complicated than the idealized ones, it is difficult to determine the parameters j and a. We can probably determine j and a in the following ways: for example, taking the average $\bar{a}$ of the mountains' height in a certain area on the actual surface by using an instrument which can measure the topography of rough surfaces, such as a laser microscope; the average $\bar{a}$ can be applied to the model instead a. Also, using the microscope, the valleys' volume can be determined by putting a hypothetical plane at proper height and angle over an actual surface, the valleys' volume ψ can be calculated under the plane. Since $\bar{a}$ and the valleys' volume ψ are determined, and from $j=\bar{a}\times\psi$, j is determined.

On the other hand, it is very difficult to determine the fluid mobility k in the valleys on both real and idealized rough surfaces. Actually, the model is useful even if the mobility k is treated as $k=0$, when the mountain height is small. We need further studies to find practical parameters to characterize real rough surfaces.

The mobility k in valleys seems actually to depend on the flow velocity of fluid, although k is considered as constant in the model. if the velocity is larger, k is expected to become smaller, namely, the mobility become small.

The relationship between surface roughness and splashing has not been understood yet. The mechanism how roughness causes splashing is also not clarified. Impact velocity might affect splashing phenomena or, more strictly, the radial expansion rate at impingement. The radial expansion rate at impact is described in Eq. 13. Substituting $h=2d_0{}^3/3D_m{}^2$ into Eq. 13, then substituting $D_m/d_0=1.06\,\mathrm{Re}^{1/6}$ into the obtained equation, the expression becomes

$$\left(\frac{dR}{dt}\right)_{t=0}=v_0\sqrt{\frac{d_0}{2h}}=v_0\frac{D_m}{d_0}\frac{\sqrt{3}}{2}=1.06\frac{\sqrt{3}}{2}\mathrm{Re}^{1/6}v_0 \qquad [37]$$

Equation 37 shows the radial expanding rate at impact is 441 m/sec in the case of a molten nickel particle as shown Table 1. In this case, the radial expansion rate is about 4.4 times the impact velocity. Although the splashing conditions are not clarified, the impact velocity might be one of the factors which cause the splashing. A larger impinging velocity has more chance of causing splash if other conditions are the same. We must note the radial flow velocity is much larger than the impact velocity. Larger impact velocity makes the expanding splat thinner, If the splat is thinner, the flattening behavior is more influenced by roughness. Therefore, the parameter jav_0/d_0 probably expresses more strictly the tendency to

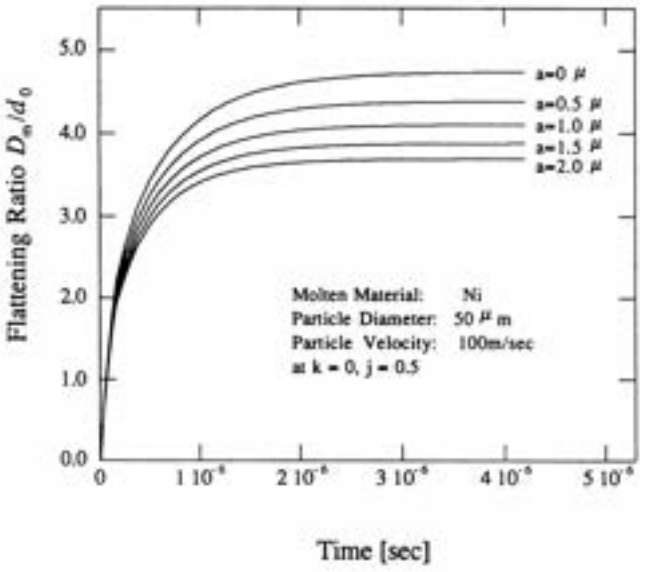

Fig. 7 The relationship between flattening ratio and time with respect to the surface roughness parameter.

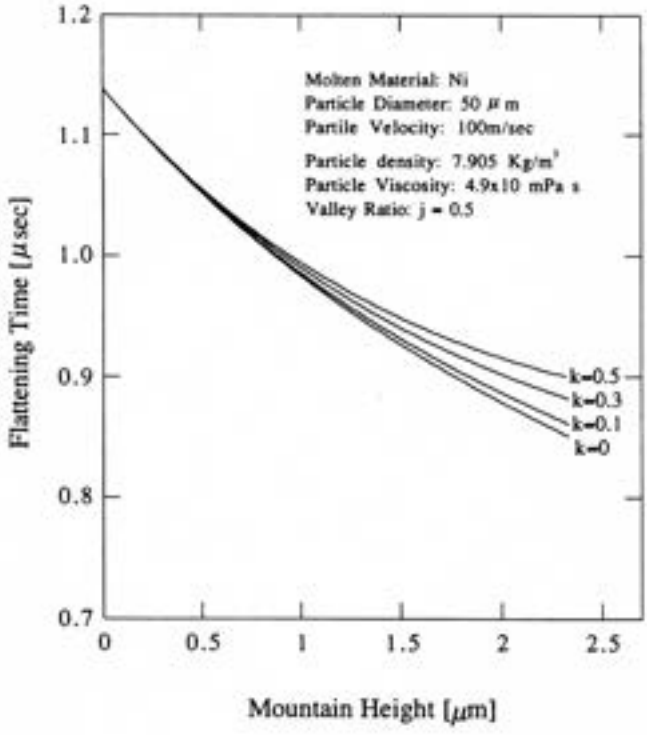

Fig. 8 The relationship between flattening time and surface roughness with respect to the fluid mobility parameter in valleys.

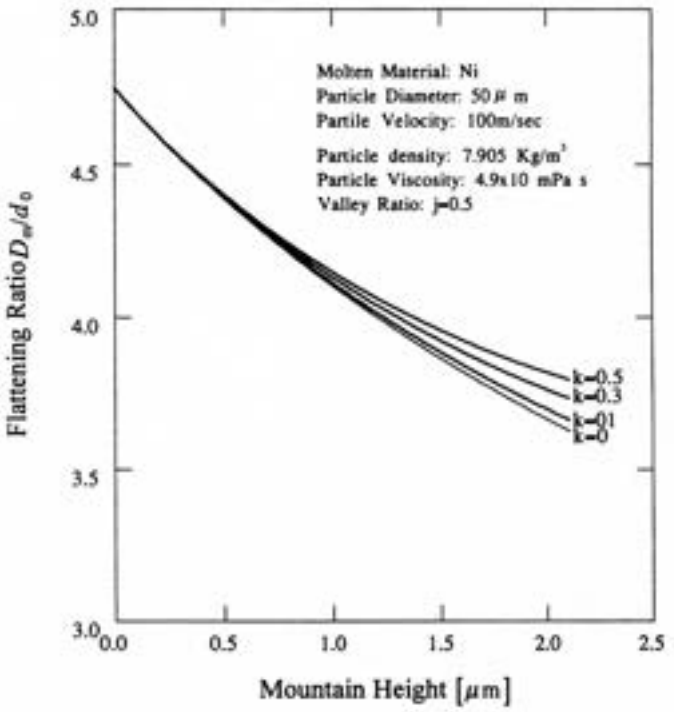

Fig. 9 The relationship between flattening ratio and surface roughness with respect to the fluid mobility parameter in valleys.

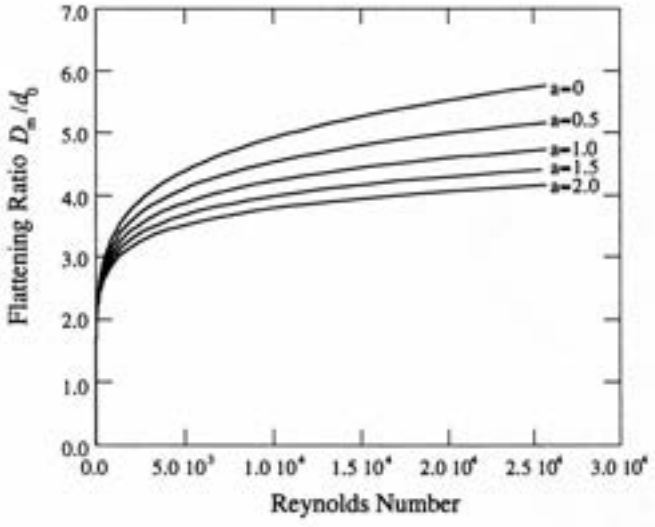

Fig. 10 The relationship between flattening ratio and Reynolds number with respect to the surface roughness parameter in the case of a molten nickel particle.

splashing than impact velocity v_0, however, the critical value is not clear.

In conclusion, a formula which describes the flattening process on rough surfaces is obtained in this study by converting the process on a rough surface to that on a smooth, flat surface as a splat consisting of two layers with different flow fields, and introducing parameters characterizing rough surfaces. This model shows the flattening ratio and the flattening time decrease with increasing roughness which have been experimentally confirmed by some studies.

References

1. O. G. Engel, Journal of Research of the National Bureau of Standards, Vol. 54(5), 281-298, May (1955).
2. F. J. Heymann, Journal of Applied Physics, Vol. 40(13), 5113-5122, December (1969).
3. J. Madejski, Int. J. Heat Mass Transfer, Vol. 19, 1009-1013, (1976).
4. G. Trapaga, J. Szekely, Metallurgical Transactions B, Volume 22B, 901-914, (1991).
5. H. Fukanuma, Journal of Thermal Spray Technology, Vol. 3(1), 33-44, March (1994).
6. H. Fukanuma and A. Ohmori, Proceedings of the 7th NTSC, Boston, Massachusetts, 563-568, June (1994).
7. J. Yankee and B. J. Plekta, Journal of Thermal Spray Technology, Vol. 2(3), 271-281, September (1993).
8. Fantassi, M. Vardelle, A. Vardelle, and P. Fauchais, Journal of Thermal Spray Technology, Vol. 2(4), 379-384, December (1993).
9. Vardelle, A. Vardelle, A.C. Leger, P. Fauchais, and D. Gobin, Journal of Thermal Spray Technology, Vol. 4(1), 50-57, March (1995).
10. ChangJiu Li, A. Ohmori and Y. Harada, Proceeding of ITSC'95, Kobe, Japan, 333-339, May (1995).
11. Fukumoto, S. Katoh and I. Okane, Proceeding of ITSC'95, Kobe, Japan, 353-358, May (1995).
12. Montavan, S. Sampath, C.C. Berndt, H. Herman and C. Coddet, Proceeding of ITSC'95, Kobe, Japan, 365-370, May (1995).
13. Montvan, C. Coddet, Proceeding of 8th NTSC, Houston, Texas, 285-289, September (1995)
14. Moreau, P. Gougeon, M. Lamontagne, Journal of Thermal Spray Technology, Vol. 4(1), 25-33 (1995)
15. Leger, M. Vardelle, A. Vardelle, B. Dussoubs, P. Fauchais, Proceedings of the 8th NTSC, Houston, Texas, 169-174, September 1995.
16. Bianchi, A. Grimaud, F. Blein, P. Lucchèe, and P. Fauchais, Journal of Thermal Spray Technology, Vol. 4(1), 59-65, March (1995)